

Sensitivity analysis of β -decay half-life predictions for Ge, As, Zr and Mo nuclei within the mapped interacting boson model

M. Homma¹ and K. Nomura^{1,2,*}

¹*Department of Physics, Hokkaido University, Sapporo 060-0810, Japan*

²*Nuclear Reaction Data Center, Hokkaido University, Sapporo 060-0810, Japan*

(Dated: April 14, 2025)

We analyze parameter sensitivities of the mapped interacting boson model (IBM) and boson-fermion-fermion model (IBFFM) in the description of β -decay properties of the even-mass neutron-deficient Ge and As, and neutron-rich Zr and Mo isotopes. Based on the self-consistent mean-field calculations with a given energy density functional and a pairing interaction, the IBM Hamiltonian for even-even nuclei, single-particle energies, and occupation probabilities for unpaired nucleons, which are necessary building blocks of the IBFFM Hamiltonian and Gamow-Teller and Fermi transition operators, are completely determined. A few coupling constants of the boson-fermion and residual neutron-proton interactions are only phenomenological parameters fitted to reproduce low-energy spectra of odd-mass and odd-odd nuclei. It is found that the calculated $\log_{10} ft$ values for the β^+ decays $^{68}\text{As} \rightarrow ^{68}\text{Ge}$ are particularly sensitive to the quadrupole-quadrupole boson interaction strength used for the parent (^{68}As) nucleus. We further incorporate higher-order terms in the one-nucleon transfer operators in the boson system, and find that, while their effects are non-negligible, they do not significantly alter qualitative features of β -decay properties. We report a novel application of the mapped IBM framework to compute β -decay half-lives, and show that the observed trend along isotopic chains are reasonably reproduced.

I. INTRODUCTION

The nuclear β decay plays a major role in the synthesis of heavy chemical elements in the early universe, and is thus of fundamental importance in nuclear physics and related fields. While light elements such as hydrogen, helium, and lithium, which have masses $A \leq 7$, are created in big-bang nucleosynthesis, and heavier elements up to iron are synthesized as stars evolve, elements heavier than iron are considered to be produced by the s and r processes, which proceed via neutron capture and β decay. The s process follows the β -stability line, and plenty of experimental data are available for the stable nuclei. On the other hand, the r process follows a path on the neutron-rich side, which is far from the stability line, and it is even more challenging to study neutron-rich heavy nuclei experimentally [1–5]. Therefore, current studies of the r process rely heavily on theoretical predictions on physical quantities such as the neutron capture cross sections and β -decay half-lives.

It is thus crucial to develop theoretical models that accurately describe characteristics of β decay, and to reduce or make controllable the possible theoretical uncertainties in given models. Nuclear structure models that are frequently applied to study the β -decay of medium-heavy and heavy nuclei include the nuclear shell model (NSM) [6–10], the quasiparticle random-phase approximation (QRPA) [11–22], and the interacting boson model (IBM) [23–35]. The basic assumption of the IBM is that collective monopole (with spin and parity $J^\pi = 0^+$) and quadrupole ($J^\pi = 2^+$) pairs of valence nucleons are approximated to s and d bosons, respectively [36], which

therefore represents a drastic truncation of the full shell-model configuration space. The IBM has been often employed in the β -decay studies in different mass regions. While the IBM is able to simultaneously describe low-lying collective states and β decays of heavy nuclei in deformed or open-shell regions, in the majority of the earlier β -decay studies within the IBM most of the model parameters were obtained from phenomenological adjustments to the experimental low-energy spectra for each nucleus. The reliability of the model in the predictions of β -decay properties of neutron-rich nuclei that are very far from the stability line and for which experimental data are not available has not yet been clarified.

In recent years a method of calculating β -decay properties has been developed [29, 30, 32, 34] that consists of mapping the self-consistent mean-field (SCMF) solutions onto the IBM [37–39]. In that method, strength parameters of the IBM Hamiltonian describing even-even nuclei are determined microscopically so that the potential energy surface (PES) obtained from the self-consistent mean-field (SCMF) calculation employing a given energy density functional (EDF) and a pairing force is mapped onto the expectation value of the boson Hamiltonian. Odd-odd nuclear systems are described in terms of the interacting boson-fermion-fermion model (IBFFM) [40, 41], which consists of the even-even (IBM) core representing the collective motion, and an unpaired neutron and an unpaired proton as single-particle degrees of freedom. The SCMF calculation provides single-particle energies and occupation probabilities for odd nucleons, which are used as a microscopic input to build the IBFFM Hamiltonian. However, only the strength parameters for the interactions between unpaired nucleons and even-even boson cores and between unpaired nucleons are determined so as to reproduce the low-lying energy

* nomura@sci.hokudai.ac.jp

spectra of each odd-odd nucleus to a certain accuracy. The wave functions of the IBM and IBFFM, which give reasonable descriptions of low-lying states of even-even and odd-odd nuclei, respectively, are used to compute Gamow-Teller (GT) and Fermi transition strengths for the β decays of interest.

In Ref. [34], in particular, the mapped IBM was applied to study β -decay properties as well as low-lying collective states of even-even and odd-odd nuclei from Kr to Cd isotopes near $N = 60$, using the relativistic EDF as a microscopic input. In that study, the observed systematic of the β -decay $\log_{10}ft$ values along isotopic chains was reproduced reasonably well, but some of the measured $\log_{10}ft$ values for those nuclei with $N \leq 60$ were significantly underestimated. To address the deficiency, in a subsequent paper [35] we studied the parameter dependence of the predicted $\log_{10}ft$ values for the β^- decay of the Zr isotopes within the EDF-mapped IBM framework. By varying IBFFM as well as IBM parameters used in Ref. [34], we found that the $\log_{10}ft$ values for the β^- decay of Zr isotopes depended strongly on the quadrupole-quadrupole boson interaction strength and that of the residual neutron-proton interaction of tensor type in the IBFFM Hamiltonian for the daughter (Nb) nuclei. Furthermore, it was found that, when these parameters were adjusted to the experimental $\log_{10}ft$ values, they led to a better reproduction of the energy spectra of the Nb isotopes and their boson core (Mo) nuclei.

In the present study, we extend the analysis of Ref. [35] to the β decay of neutron-deficient Ge and As nuclei in the mass $A \approx 70$ region to see if the conclusion drawn in Ref. [35] is valid in other mass regions. As a representative case, we specifically consider the β^+ decay of ^{68}As . We also incorporate higher-order terms in the one-nucleon transfer operators in the IBFFM in constructing the GT and Fermi transition operators, and study the role played by these terms in the corresponding matrix elements for the β^+ decays of $^{68,70}\text{As}$, and β^- decays of ^{78}Ge , and even-even $^{98-110}\text{Zr}$ and $^{102-110}\text{Mo}$ isotopes. Here, the choice of the specific regions $A \approx 70$ and $A \approx 100$ is motivated by fact that they are rather close to ^{76}Ge , ^{96}Zr , and ^{100}Mo , which are candidate nuclei for the neutrinoless double- β decay, a fundamental nuclear decay under extensive investigations [42–44].

We further report a novel application of the mapped IBM framework to compute β -decay half-lives of the considered Ge, As, Zr, and Mo isotopes. While the β -decay half-lives are extensively studied by various theoretical approaches such as NSM and QRPA, the IBM has mostly been applied to compute the GT and Fermi transitions to only a few low-lying states. An exception is perhaps the IBM-2 calculations of the double- β decay nuclear matrix elements in Refs. [27, 45, 46], where a number of intermediate states of odd-odd nuclei were computed without the closure approximation. To the best of our knowledge, the application of the IBM to systematic half-life studies for neutron-rich isotopes has rarely been attempted.

The paper is organized as follows. Section II provides

TABLE I. Configurations of the odd-odd nuclei under study (first column) with their neutron numbers N (second column). Corresponding even-even boson core nuclei are shown in the third column. The fourth (fifth) column shows whether the odd neutron (proton) is of particle (p) or hole (h) nature.

Odd-odd	N	Even-even core	Neutron	Proton
$^{33}\text{As}_N$	$35 \leq N \leq 39$	$^{32}\text{Ge}_{N-1}$	p	p
$^{33}\text{As}_N$	$41 \leq N \leq 45$	$^{32}\text{Ge}_{N+1}$	h	p
$^{41}\text{Nb}_N$	$55 \leq N \leq 65$	$^{42}\text{Mo}_{N-1}$	p	h
	$N = 67, 69$	$^{42}\text{Mo}_{N+1}$	h	h
$^{43}\text{Tc}_N$	$55 \leq N \leq 65$	$^{44}\text{Ru}_{N-1}$	p	h
	$N = 67$	$^{44}\text{Ru}_{N+1}$	h	h

a brief reminder of the EDF-mapped IBM and IBFFM methods, and calculated results for low-energy spectra of even-mass nuclei. In Sec. III β -decay properties are discussed, including the parameter sensitivity of the ^{68}As β^+ decay, effects of the higher-order terms, and predictions on the half-lives. Section IV gives a summary of the principal results and perspectives for future studies.

II. MAPPED IBM-2 AND IBFFM-2

This section describes the procedure to construct the IBFFM Hamiltonian from the EDF calculation, gives definitions of the GT and Fermi operators, and presents calculated results for low-energy spectra.

A. Model Hamiltonian

As in the previous studies of Refs. [34, 35], we use the neutron-proton IBM (IBM-2) and IBFFM (IBFFM-2). The building blocks of the IBM-2 are neutron s_ν and d_ν bosons, and proton s_π and d_π bosons. The s_ν and d_ν (s_π and d_π) bosons are associated with the collective monopole and quadrupole pairs of valence neutrons (protons), respectively [36, 47, 48]. We adopt the IBM-2 Hamiltonian of the same form as used in Refs. [34, 35]:

$$\begin{aligned} \hat{H}_B = & \epsilon_d(\hat{n}_{d_\nu} + \hat{n}_{d_\pi}) + \kappa \hat{Q}_\nu \cdot \hat{Q}_\pi \\ & + \kappa_\nu \hat{Q}_\nu \cdot \hat{Q}_\nu + \kappa_\pi \hat{Q}_\pi \cdot \hat{Q}_\pi + \kappa' \hat{L} \cdot \hat{L}. \end{aligned} \quad (1)$$

$\hat{n}_{d_\rho} = \hat{d}_\rho^\dagger \cdot \tilde{d}_\rho$ ($\rho = \nu$ or π) denotes the d -boson number operator with $\tilde{d}_{\rho\mu} = (-1)^\mu d_{\rho-\mu}$, and ϵ_d is the single d boson energy relative to that of s bosons. The second, third, and fourth terms are the quadrupole-quadrupole interactions between neutron and proton bosons, between neutron and neutron bosons, and between proton and proton bosons, respectively. The quadrupole operator \hat{Q}_ρ is defined as $\hat{Q}_\rho = s_\rho^\dagger \tilde{d}_\rho + \tilde{d}_\rho^\dagger s_\rho + \chi_\rho (d_\rho^\dagger \times \tilde{d}_\rho)^{(2)}$, where χ_ν and χ_π are dimensionless parameters. κ , κ_ν , and κ_π are strength parameters of the quadrupole-quadrupole interactions. The last term of Eq. (1) stands for a rotational term, with κ' being the strength parameter, and

$\hat{L} = \hat{L}_\nu + \hat{L}_\pi$ denotes the angular momentum operator with $\hat{L}_\rho = (\hat{d}_\rho^\dagger \times \hat{d}_\rho)^{(1)}$.

The IBFFM-2 Hamiltonian is given in general by

$$\hat{H} = \hat{H}_B + \hat{H}_F^\nu + \hat{H}_F^\pi + \hat{V}_{BF}^\nu + \hat{V}_{BF}^\pi + \hat{V}_{\nu\pi}. \quad (2)$$

The first term represents the IBM-2 core Hamiltonian of Eq. (1). The second (third) term of Eq. (2) represents the single-neutron (proton) Hamiltonian of the form

$$\hat{H}_F^\rho = - \sum_{j_\rho} \epsilon_{j_\rho} \sqrt{2j_\rho + 1} (a_{j_\rho}^\dagger \times \tilde{a}_{j_\rho})^{(0)} \equiv \sum_{j_\rho} \epsilon_{j_\rho} \hat{n}_{j_\rho}, \quad (3)$$

where ϵ_{j_ρ} stands for the single-particle energy of the odd neutron or proton orbital j_ρ . $a_{j_\rho}^{(\dagger)}$ represents the particle annihilation (creation) operator, with \tilde{a}_{j_ρ} defined by $\tilde{a}_{j_\rho m_\rho} = (-1)^{j_\rho - m_\rho} a_{j_\rho - m_\rho}$. On the right-hand side of Eq. (3), \hat{n}_{j_ρ} stands for the number operator for the odd particle. The single-particle space for the As isotopes taken in the present study comprises the neutron and

proton $2p_{1/2}$, $2p_{3/2}$, and $1f_{5/2}$ orbitals. The space for the Nb and Tc isotopes consists of the neutron $3s_{1/2}$, $2d_{3/2}$, $2d_{5/2}$, and $1g_{7/2}$ orbitals, and the proton $1g_{9/2}$ orbital. For $^{96-110}\text{Nb}$ ($^{98-110}\text{Tc}$), since the valence neutrons and protons are, respectively, treated as particles and holes, the corresponding even-even boson cores are the $^{96-110}\text{Mo}$ ($^{98-110}\text{Ru}$) nuclei, respectively. Configurations of the odd-odd $^{68-78}\text{As}$, $^{96-110}\text{Nb}$ and $^{98-110}\text{Tc}$ in terms of the boson core plus odd nucleons are summarized in Table I.

The fourth (fifth) term of Eq. (2) denotes the interaction between a single neutron (or proton) and the even-even boson core, and is given as [40, 49]

$$\hat{V}_{BF}^\rho = \Gamma_\rho \hat{V}_{\text{dyn}}^\rho + \Lambda_\rho \hat{V}_{\text{exc}}^\rho + A_\rho \hat{V}_{\text{mon}}^\rho, \quad (4)$$

where the first, second, and third terms represent the quadrupole dynamical, exchange, and monopole interactions, respectively, with the strength parameters Γ_ρ , Λ_ρ , and A_ρ . Within the generalized seniority framework [40, 49], the terms in (4) are expressed of the forms

$$\hat{V}_{\text{dyn}}^\rho = \sum_{j_\rho j'_\rho} \gamma_{j_\rho j'_\rho} (a_{j_\rho}^\dagger \times \tilde{a}_{j'_\rho})^{(2)} \cdot \hat{Q}_{\rho'}, \quad (5)$$

$$\hat{V}_{\text{exc}}^\rho = - \left(s_{\rho'}^\dagger \times \tilde{d}_{\rho'} \right)^{(2)} \cdot \sum_{j_\rho j'_\rho j''_\rho} \sqrt{\frac{10}{N_\rho(2j_\rho + 1)}} \beta_{j_\rho j'_\rho} \beta_{j''_\rho j_\rho} : \left[(d_\rho^\dagger \times \tilde{a}_{j'_\rho})^{(j_\rho)} \times (a_{j'_\rho}^\dagger \times \tilde{s}_\rho)^{(j'_\rho)} \right]^{(2)} : + (\text{H.c.}), \quad (6)$$

$$\hat{V}_{\text{mon}}^\rho = \hat{n}_{d_\rho} \hat{n}_{j_\rho}, \quad (7)$$

where the j -dependent factors $\gamma_{j_\rho j'_\rho} = (u_{j_\rho} u_{j'_\rho} - v_{j_\rho} v_{j'_\rho}) Q_{j_\rho j'_\rho}$ and $\beta_{j_\rho j'_\rho} = (u_{j_\rho} v_{j'_\rho} + v_{j_\rho} u_{j'_\rho}) Q_{j_\rho j'_\rho}$, with $Q_{j_\rho j'_\rho} = \langle \ell_\rho \frac{1}{2} j_\rho || Y^{(2)} || \ell'_\rho \frac{1}{2} j'_\rho \rangle$ being the matrix element of the fermion quadrupole operator in the single-particle basis. $\hat{Q}_{\rho'}$ in Eq. (5) denotes the quadrupole operator in the boson system, introduced in Eq. (1). The notation $:(\dots):$ in Eq. (6) stands for normal ordering. Furthermore, the unperturbed single-particle energy, ϵ_{j_ρ} , in Eq. (3) is replaced with the quasiparticle energy $\tilde{\epsilon}_{j_\rho}$.

$\hat{V}_{\nu\pi}$ in (2) corresponds to the residual interaction between the unpaired neutron and proton. In this study, we consider the following form:

$$\begin{aligned} \hat{V}_{\nu\pi} = & 4\pi v_d \delta(\mathbf{r}) \delta(\mathbf{r}_\nu - \mathbf{r}_0) \delta(\mathbf{r}_\pi - \mathbf{r}_0) \\ & - \frac{1}{\sqrt{3}} v_{\text{ss}} \boldsymbol{\sigma}_\nu \cdot \boldsymbol{\sigma}_\pi + v_t \left[\frac{3(\boldsymbol{\sigma}_\nu \cdot \mathbf{r})(\boldsymbol{\sigma}_\pi \cdot \mathbf{r})}{r^2} - \boldsymbol{\sigma}_\nu \cdot \boldsymbol{\sigma}_\pi \right]. \end{aligned} \quad (8)$$

The first, second and third terms stand for the δ , the spin-spin, and tensor interactions, with v_d , v_{ss} and v_t being strength parameters, respectively. Note that $\mathbf{r} = \mathbf{r}_\nu - \mathbf{r}_\pi$ is the relative coordinate of the neutron and proton, and $r_0 = 1.2A^{1/3}$ fm. The matrix element of $\hat{V}_{\nu\pi}$ depends on

the occupation v_j and unoccupation u_j amplitudes.

B. Procedure to build the IBFFM-2 Hamiltonian

The procedure to determine the IBFFM-2 Hamiltonian Eq. (2) consists of the following three steps.

1. The constrained SCMF calculations are performed for the even-even Ge, Zr, Mo, and Ru isotopes by means of the relativistic Hartree-Bogoliubov (RHB) method [50, 51], using the density-dependent point-coupling (DD-PC1) EDF [52] and the separable pairing force of finite range [53]. The SCMF calculations yield PESs with triaxial quadrupole (β and γ) shape degrees of freedom. The RHB-SCMF PES is then mapped onto the expectation value of \hat{H}_B in the boson coherent state [54], and this procedure specifies the IBM-2 Hamiltonian parameters [37, 38]. Only the parameter κ' is determined separately by comparing cranking moments of inertia between fermionic and bosonic systems [39]. In addition, it is assumed that $\kappa_\nu = \kappa_\pi = \kappa/2$ for the even-even $^{96-110}\text{Zr}$ nu-

clei and $\kappa_\nu = \kappa_\pi = 0$ MeV for all the other nuclei, for simplicity.

2. The single-fermion Hamiltonian \hat{H}_F (3) and boson-fermion interactions \hat{V}_{BF} (4) are constructed by using the procedure of Refs. [55, 56]: The RHB-SCMF calculations are performed for the neighboring odd- N or odd- Z nucleus with the constraint on zero deformation to provide quasiparticle energies, $\tilde{\epsilon}_{j_\rho}$, and occupation probabilities, $v_{j_\rho}^2$, at the spherical configuration for the odd nucleon at orbitals j_ρ . These quantities are then input to \hat{H}_F and \hat{V}_{BF} , respectively. The remaining three coupling constants, Γ_ρ , Λ_ρ , and A_ρ , are determined to fit the experimental data for a few low-lying positive-parity levels of each odd- N and odd- Z nuclei.
3. The parameters Γ_ρ , Λ_ρ , and A_ρ , which are determined in the previous step for the neighboring odd- N and odd- Z nuclei, are used for the odd-odd nucleus, in order to reduce the number of parameters. The quasiparticle energies $\tilde{\epsilon}_{j_\rho}$ and occupation probabilities $v_{j_\rho}^2$ are, however, newly computed for the odd-odd nucleus in the same way as in the previous step, that is, by the SCMF calculations constrained to zero deformation, since it is more realistic to use these values specifically calculated for the odd-odd nucleus than to reuse the corresponding values for the neighboring odd-mass nuclei. Then, the parameters of $\hat{V}_{\nu\pi}$ (8) are fixed to reproduce, to a certain accuracy, the observed low-lying positive-parity levels of each odd-odd nucleus.

The strength parameters for the IBFFM-2 determined by the above procedure for the even-even Ge and odd-odd As nuclei are found in Table I of Ref. [32]. While the parameters for the even-even Zr and Mo and odd-odd Tc and Nb isotopes with the neutron numbers $54 \leq N \leq 64$ were already presented in Ref. [34] (Fig. 3 and Table II), since we extend the calculations beyond $N = 64$, we show in Figs. 1 and 2 the IBM-2 and IBFFM-2 parameters for all the considered Zr, Mo, Nb, and Tc nuclei, for the sake of completeness.

C. Calculated low-energy spectra

Figure 3 depicts the calculated excitation energies for low-lying states of the even-even nuclei $^{68-78}\text{Ge}$, $^{96-110}\text{Zr}$, and $^{98-110}\text{Mo}$, and odd-odd nuclei $^{68-78}\text{As}$, $^{96-110}\text{Nb}$, and $^{98-110}\text{Tc}$, obtained from the diagonalizations of the IBM-2 and IBFFM-2 Hamiltonians, respectively. The experimental data, available in the NNDC database [57], are also included in the plots. The calculated excitation energies for the even-mass Ge and As, shown in Figs. 3(a) and 3(g), are taken from those in Figs. 3 and 4 of Ref. [32], without any modification. The predicted energies for the even-even Zr and Mo, and

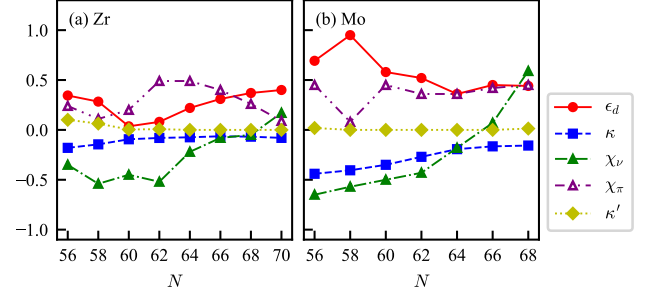


FIG. 1. The IBM-2 parameters for the even-even (a) $^{96-110}\text{Zr}$ and (b) $^{98-110}\text{Mo}$ nuclei, which are obtained from mapping the RHB-SCMF onto the IBM-2 deformation energy surfaces.

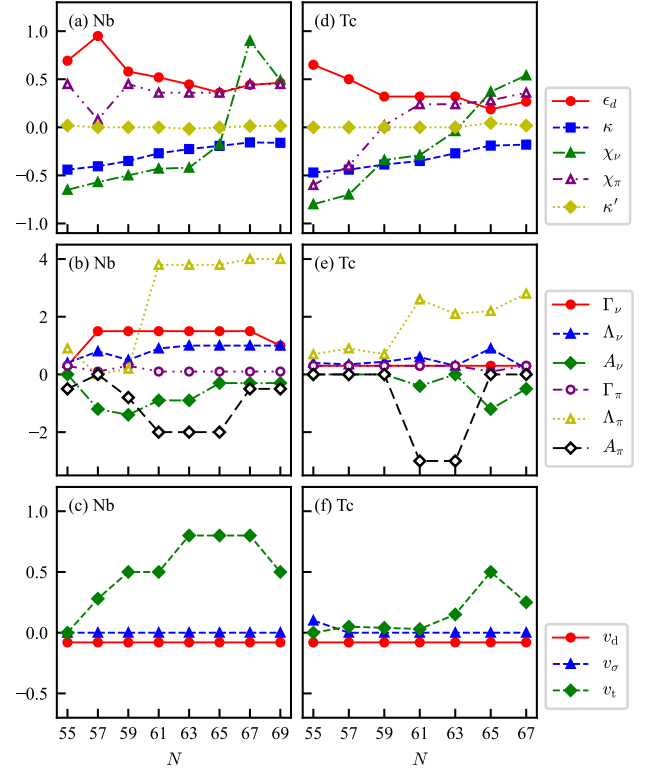


FIG. 2. The IBFFM-2 parameters adopted in the present study for the odd-odd $^{96-110}\text{Nb}$ (left column) and $^{98-110}\text{Tc}$ (right column) nuclei.

odd-odd Nb and Tc isotopes with neutron number up to $N = 64$, shown in Figs. 3(c), 3(e), 3(i), and 3(k), are taken from Figs. 2 and 5 of Ref. [34]. An update to the previous studies [32, 34] is therefore the inclusion of the results for those Zr, Mo, Nb, and Tc isotopes with $N \geq 66$. In addition, the calculated 6_1^+ energy levels for both the even-even and odd-odd nuclei are here included, which were not considered in Refs. [32, 34].

What is particularly noteworthy in Fig. 3 is a drastic change of calculated energy levels for the neutron-rich

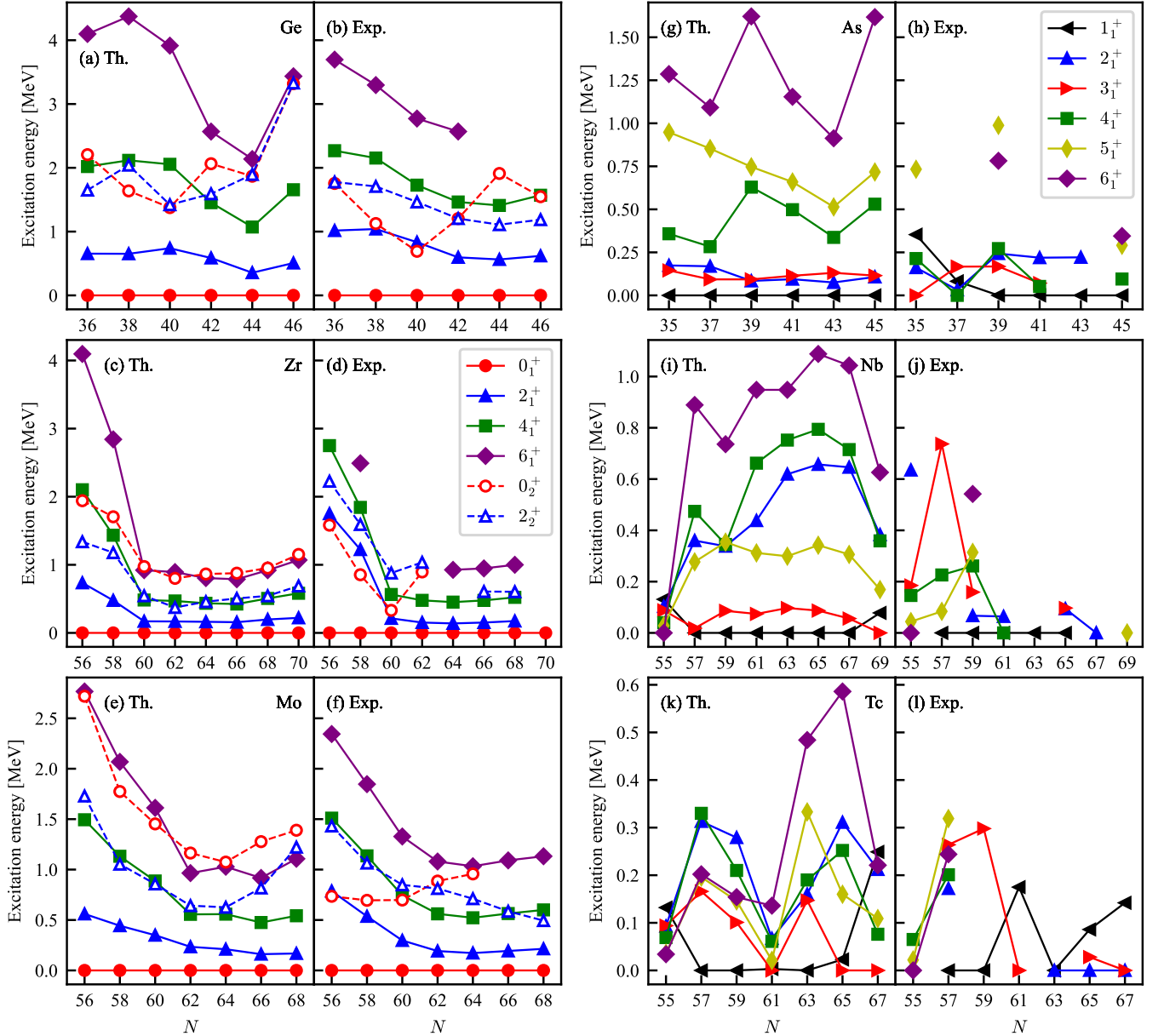


FIG. 3. Excitation energies of the even-even $^{68-78}\text{Ge}$, $^{96-110}\text{Zr}$ and $^{98-110}\text{Mo}$ nuclei (first and second columns), and odd-odd $^{68-78}\text{As}$, $^{96-110}\text{Nb}$ and $^{98-110}\text{Tc}$ nuclei (third and fourth columns) as functions of the neutron number N . Calculated energies are plotted in the first and third columns, and are compared with the experimental data [57], shown in the second and fourth columns.

Zr and Mo isotopes near $N = 60$, indicating a quantum phase transition (QPT) in nuclear shapes [58]. For $N > 60$ the predicted ground-state yrast levels, i.e., 2_1^+ , 4_1^+ , and 6_1^+ , for the Zr and Mo nuclei become compressed in energy, resembling a rotational band. This low-lying structure appears to continue toward $N = 70$. The mapped IBM-2 reproduces this trend of the yrast levels well, but overestimates the non-yrast 0_2^+ and 2_2^+ levels for $N \geq 60$. For instance, while the measured 2_2^+ level for the even-even Mo isotopes keeps decreasing with N , which may indicate a shape coexistence effect or

pronounced γ -softness, the mapped IBM-2 rather suggests an increase of this level for $N > 64$ [see Fig. 3(e)]. In general, the overestimation of the non-yrast levels in the mapped IBM-2 framework has been explained by the too large quadrupole-quadrupole interaction strength κ , which is derived from the EDF-to-IBM PES mapping, or by the fact that the calculation does not include configuration mixing of normal and intruder states [59], which are related to coexisting mean-field minima on the PES.

As for the odd-odd nuclei, especially the neutron-rich Nb and Tc, it is difficult to determine the IBFFM-

2 strength parameters, as the experimental data for the low-energy spectra are scarce. Here they are determined mainly to reproduce the spin of the ground state, or extrapolated from the neighboring odd-odd nuclei where spectroscopic data are available. As one can see in Figs. 3(i)–3(l), there appear notable changes in the calculated low-energy level structure near the phase-transitional region $N \approx 60$, e.g., from ^{96}Nb ($N = 55$) to ^{104}Nb ($N = 63$), and from ^{98}Tc ($N = 55$) to ^{106}Tc ($N = 63$). These behaviors of low-energy levels in the odd-odd systems reflect, to a large extent, the structural evolution in the adjacent even-even nuclei.

We do not, however, go into further details about the nuclear structure aspects of these nuclei, since the scope of the present paper is rather to investigate their β -decay properties. More thorough discussions about the calculated excitation energies, including the comparisons with experimental data in the context of the shape QPT and coexistence and possible remedies of the deficiencies of the model descriptions, can be found in Refs. [32, 34].

III. β DECAY

A. Gamow-Teller and Fermi operators

The Gamow-Teller \hat{T}^{GT} and Fermi \hat{T}^{F} transition operators are here defined by

$$\hat{T}^{\text{GT}} = \sum_{j\nu j\pi} \eta_{j\nu j\pi}^{\text{GT}} \left(\hat{P}_{j\nu} \times \hat{P}_{j\pi} \right)^{(1)}, \quad (9)$$

$$\hat{T}^{\text{F}} = \sum_{j\nu j\pi} \eta_{j\nu j\pi}^{\text{F}} \left(\hat{P}_{j\nu} \times \hat{P}_{j\pi} \right)^{(0)}, \quad (10)$$

respectively, with the coefficients η being

$$\eta_{j\nu j\pi}^{\text{GT}} = -\frac{1}{\sqrt{3}} \left\langle \ell_\nu \frac{1}{2} j_\nu \left\| \boldsymbol{\sigma} \right\| \ell_\pi \frac{1}{2} j_\pi \right\rangle \delta_{\ell_\nu \ell_\pi}, \quad (11)$$

$$\eta_{j\nu j\pi}^{\text{F}} = -\sqrt{2j_\nu + 1} \delta_{j\nu j\pi}. \quad (12)$$

$\hat{P}_{j\rho}$ in Eqs. (9) and (10) is identified as one of the one-particle creation operators

$$A_{j\rho m_{j\rho}}^\dagger = \zeta_{j\rho} a_{j\rho m_{j\rho}}^\dagger + \sum_{j'_\rho} \zeta_{j\rho j'_\rho} s_\rho^\dagger (\tilde{d}_\rho \times a_{j'_\rho}^\dagger)_{m_{j\rho}}^{(j_\rho)}, \quad (13)$$

$$B_{j\rho m_{j\rho}}^\dagger = \theta_{j\rho} s_\rho^\dagger \tilde{a}_{j\rho m_{j\rho}} + \sum_{j'_\rho} \theta_{j\rho j'_\rho} (d_\rho^\dagger \times \tilde{a}_{j'_\rho})_{m_{j\rho}}^{(j_\rho)}, \quad (14)$$

and the annihilation operators

$$\tilde{A}_{j\rho m_{j\rho}} = (-1)^{j_\rho - m_{j\rho}} A_{j\rho - m_{j\rho}}, \quad (15)$$

$$\tilde{B}_{j\rho m_{j\rho}}^\dagger = (-1)^{j_\rho - m_{j\rho}} B_{j\rho - m_{j\rho}}. \quad (16)$$

Note that the operators in Eqs. (13) and (15) conserve the boson number, whereas those in Eqs. (14) and (16) do not. The \hat{T}^{GT} and \hat{T}^{F} operators are constructed as

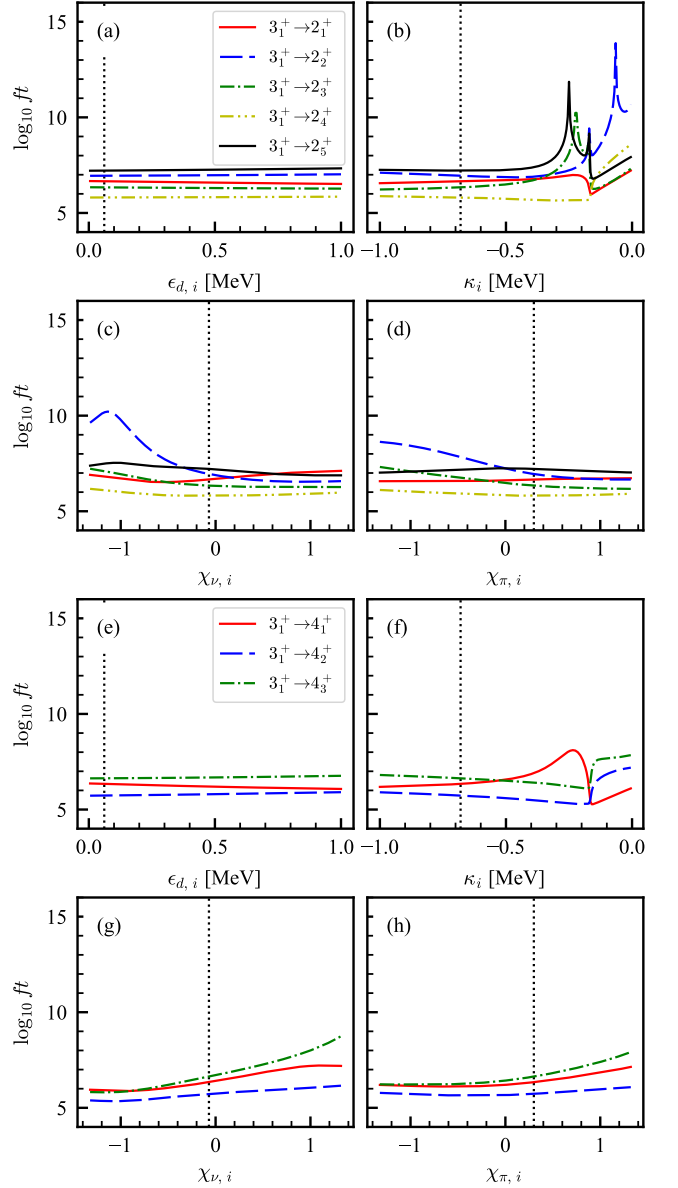


FIG. 4. Predicted $\log_{10} ft$ values for the ^{68}As β decay as functions of the boson-core parameters for the odd-odd parent ^{68}As nucleus. The vertical dotted line in each panel indicates the value of the parameter obtained from the RHB-to-IBM mapping procedure.

an appropriate combination of two of the operators in Eqs. (13)–(16), according to the type of the β decay under study (i.e., β^- or β^+) and on the particle or hole nature of bosons as well as odd nucleons. To be specific, $\hat{P}_{j\rho}$'s considered in the present for the different β -decay processes are as follows:

$$\hat{P}_{j\nu} = B_{j\nu m_{j\nu}}^\dagger, \quad \hat{P}_{j\pi} = \tilde{A}_{j\pi m_\pi} \quad (17)$$

for the $^{68,70}\text{As} \rightarrow ^{68,70}\text{Ge}$ β^+ decays,

$$\hat{P}_{j\nu} = A_{j\nu m_{j\nu}}^\dagger, \quad \hat{P}_{j\pi} = A_{j\pi m_\pi}^\dagger \quad (18)$$

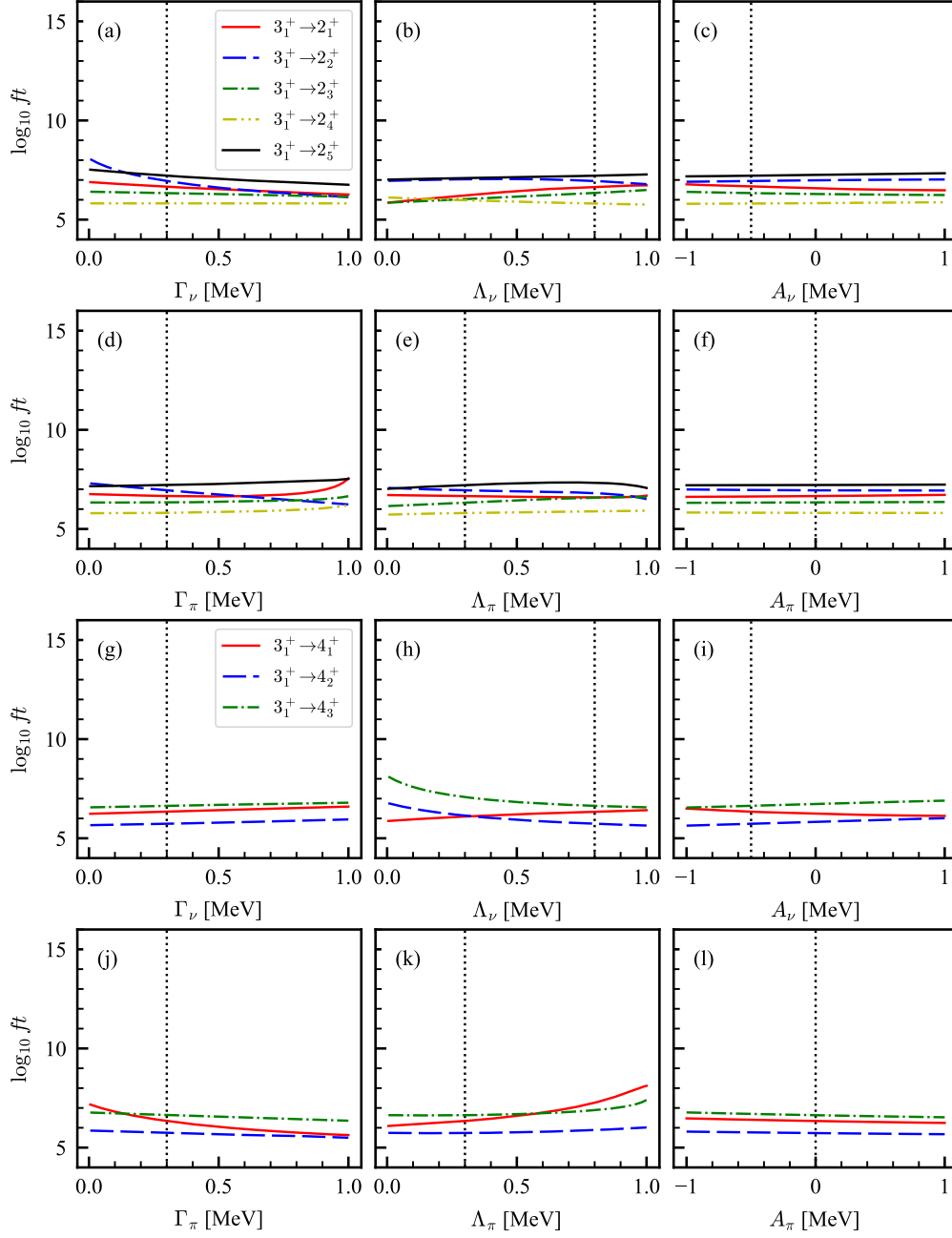


FIG. 5. Same as Fig. 4, but as functions of the interaction strengths between the odd nucleon and even-even boson core for the odd-odd parent ^{68}As nucleus.

for the $^{78}\text{Ge} \rightarrow ^{78}\text{As}$ β^- decay,

$$\hat{P}_{j\nu} = \tilde{B}_{j\nu m_\nu} \quad , \quad \hat{P}_{j\pi} = \tilde{B}_{j\pi m_\pi} \quad (19)$$

for the $^{96-106}\text{Zr} \rightarrow ^{96-106}\text{Nb}$ and $^{98-108}\text{Mo} \rightarrow ^{98-108}\text{Tc}$ β^- decays, and

$$\hat{P}_{j\nu} = A_{j\nu m_\nu}^\dagger \quad , \quad \hat{P}_{j\pi} = \tilde{B}_{j\pi m_\pi} \quad (20)$$

for the $^{108,110}\text{Zr} \rightarrow ^{108,110}\text{Nb}$ and $^{110}\text{Mo} \rightarrow ^{110}\text{Tc}$ β^- decays. It is also noted that the expressions in Eqs. (13)–

(16) are of simplified forms of the most general one-particle transfer operators in the boson representation.

Within the generalized seniority scheme [24, 60, 61], the coefficients ζ_j , $\zeta_{jj'}$, θ_j and $\theta_{jj'}$ in Eqs. (13) and (14)

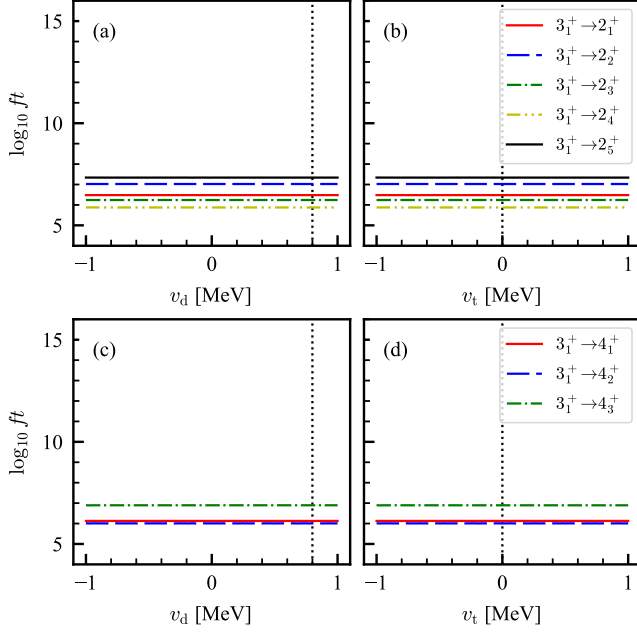


FIG. 6. Same as Fig. 4, but as functions of the strengths parameters for the residual neutron-proton interactions for the odd-odd parent ^{68}As nucleus.

can be given by

$$\zeta_{j_\rho} = u_{j_\rho} \frac{1}{K'_{j_\rho}}, \quad (21)$$

$$\zeta_{j_\rho j'_\rho} = -v_{j_\rho} \beta_{j'_\rho j_\rho} \sqrt{\frac{10}{N_\rho(2j_\rho + 1)}} \frac{1}{K K'_{j'_\rho}}, \quad (22)$$

$$\theta_{j_\rho} = \frac{v_{j_\rho}}{\sqrt{N_\rho}} \frac{1}{K''_{j_\rho}}, \quad (23)$$

$$\theta_{j_\rho j'_\rho} = u_{j_\rho} \beta_{j'_\rho j_\rho} \sqrt{\frac{10}{2j_\rho + 1}} \frac{1}{K K''_{j'_\rho}}. \quad (24)$$

The factors K , K'_{j_ρ} and K''_{j_ρ} are defined as

$$K = \left(\sum_{j_\rho j'_\rho} \beta_{j'_\rho j_\rho}^2 \right)^{1/2}, \quad (25)$$

$$K'_{j_\rho} = \left[1 + 2 \left(\frac{v_{j_\rho}}{u_{j_\rho}} \right)^2 \frac{\langle (\hat{n}_{s_\rho} + 1) \hat{n}_{d_\rho} \rangle_{0_1^+}}{N_\rho(2j_\rho + 1)} \frac{\sum_{j'_\rho} \beta_{j'_\rho j_\rho}^2}{K^2} \right]^{1/2}, \quad (26)$$

$$K''_{j_\rho} = \left[\frac{\langle \hat{n}_{s_\rho} \rangle_{0_1^+}}{N_\rho} + 2 \left(\frac{u_{j_\rho}}{v_{j_\rho}} \right)^2 \frac{\langle \hat{n}_{d_\rho} \rangle_{0_1^+}}{2j_\rho + 1} \frac{\sum_{j'_\rho} \beta_{j'_\rho j_\rho}^2}{K^2} \right]^{1/2}, \quad (27)$$

where \hat{n}_{s_ρ} is the number operator for s_ρ bosons and $\langle \cdots \rangle_{0_1^+}$ represents the expectation value of a given operator in the 0_1^+ ground state of the even-even nucleus. The

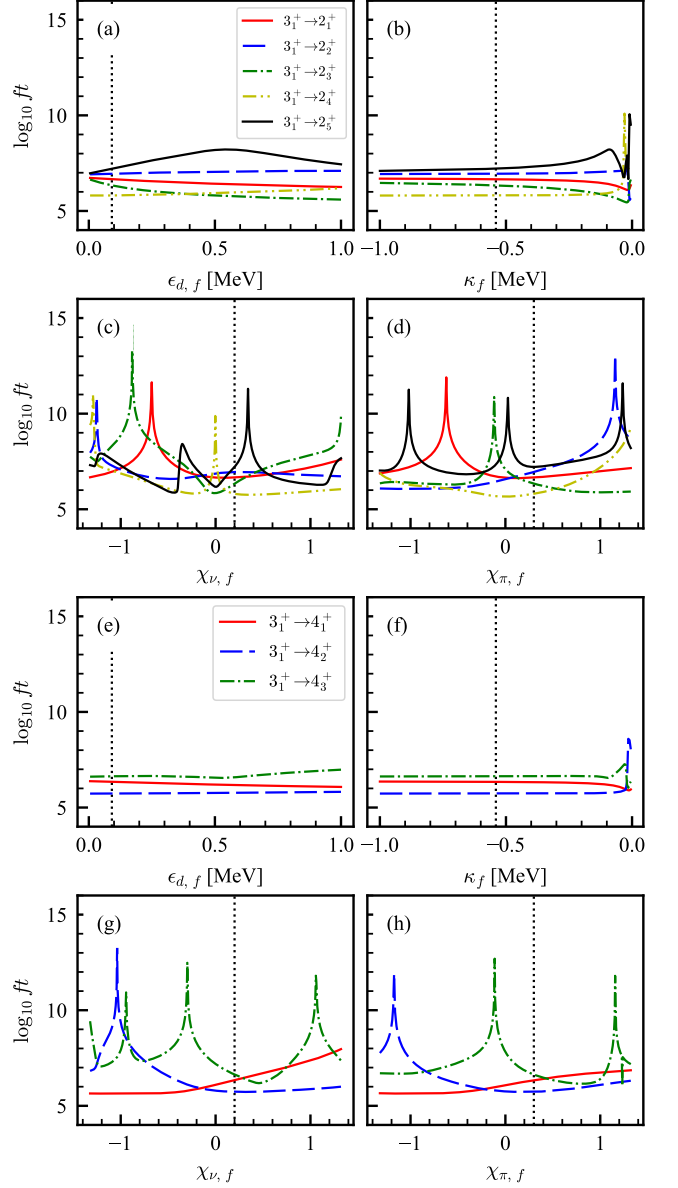


FIG. 7. Same as Fig. 4, but as functions of the IBM-2 parameters for the even-even daughter ^{68}Ge nucleus.

expressions in Eqs. (21)–(24) are specified only by the occupation v_{j_ρ} and unoccupation u_{j_ρ} amplitudes computed by the RHB-SCMF calculations, and the same (u_{j_ρ}, v_{j_ρ}) values as those used in the IBFFM-2 calculations for the odd-odd nuclei are employed. No phenomenological parameter is introduced in the \hat{T}^{GT} and \hat{T}^{F} operators.

The ft values are calculated by using the Fermi, $M_{\text{F}} = \langle I_f || \hat{T}^{\text{F}} || I_i \rangle$, and GT, $M_{\text{GT}} = \langle I_f || \hat{T}^{\text{GT}} || I_i \rangle$, reduced matrix elements for the transitions between the initial state I_i of the parent nucleus and the final state I_f of the

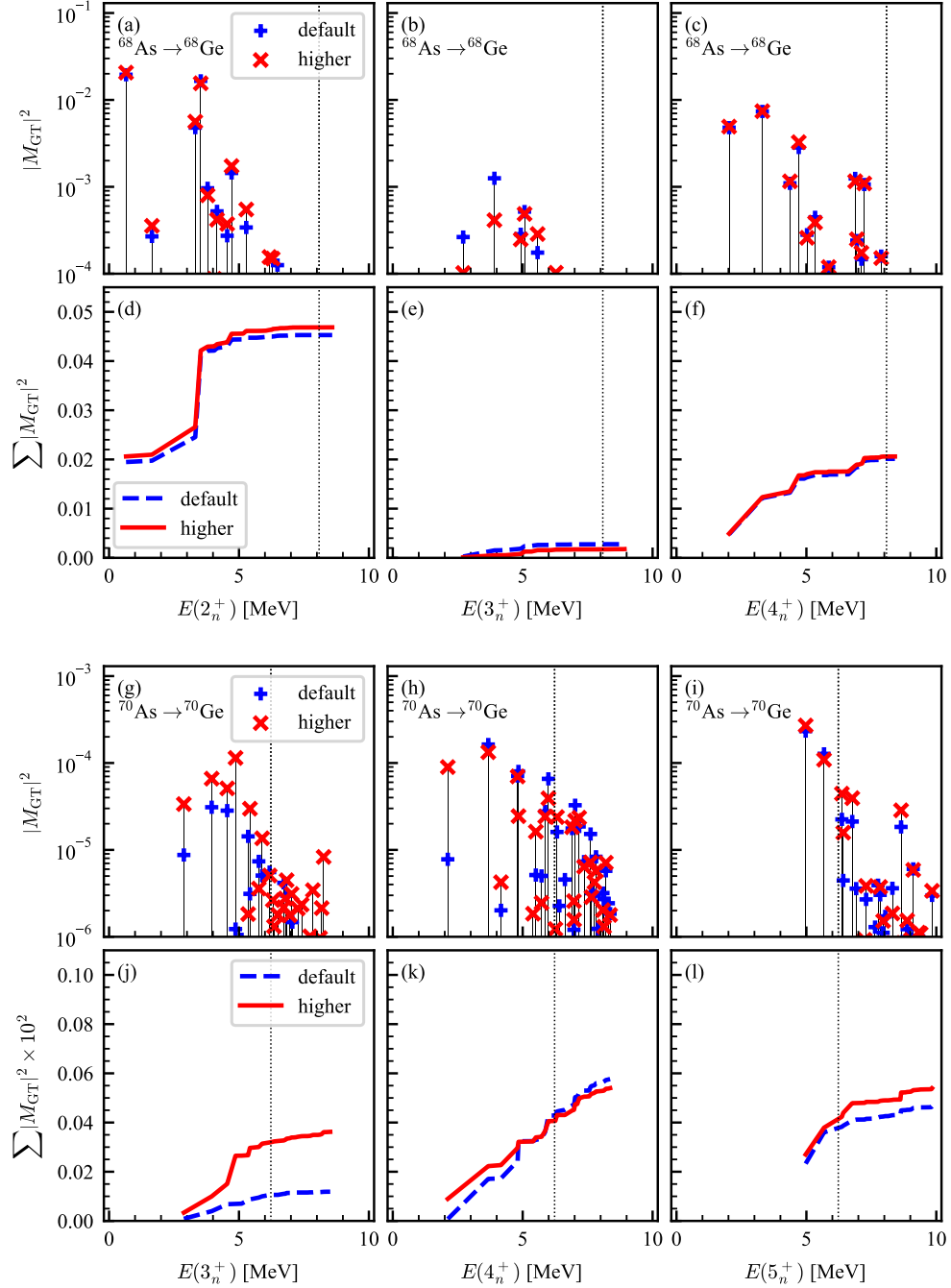


FIG. 8. Absolute squares of the calculated GT transition matrix elements, $|M_{GT}|^2$, and their running sums for the $^{68}\text{As}(3_1^+)$ and $^{70}\text{As}(4_1^+)$ β^+ decays as functions of the excitation energies $E(J_n^\pi)$ of all those final states with spin parity J^π obtained from the IBM-2. Results of two sets of the IBM-2 calculations, which do (“higher”) and do not (“default”) include the higher-order terms in the one-nucleon transfer operators, are shown. The vertical dotted line depicted in each panel stands for the experimental β -decay Q -value [57].

daughter nucleus:

$$ft = \frac{K}{|M_F|^2 + (g_A/g_V)^2 |M_{GT}|^2}, \quad (28)$$

with the factor $K = 6163$ (in seconds), $g_A = 1.27$ and $g_V = 1$ being the axial-vector and vector coupling constants, respectively.

For a more detailed account on the formalism of the

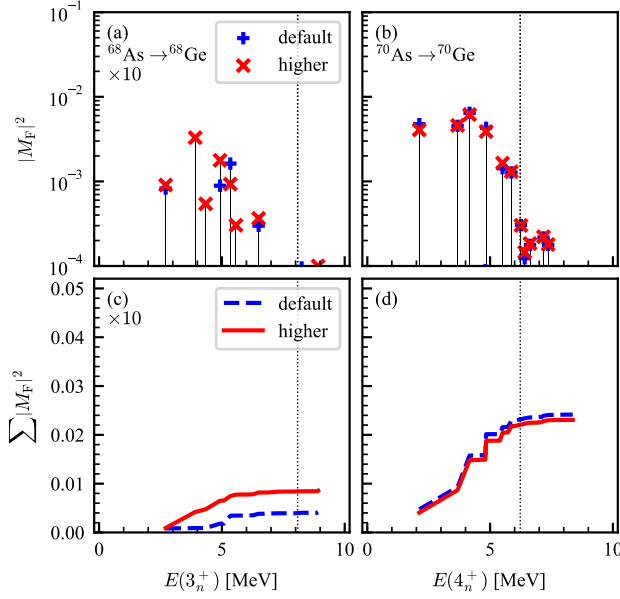


FIG. 9. Same as Fig. 8, but the calculated Fermi transition matrix elements, $|M_F|^2$.

β -decay operators within the IBFFM-2, the reader is referred to Refs. [24, 60, 61].

B. Parameter dependence of β -decay $\log_{10}ft$ of ^{68}As

As mentioned in Sec. II A, the independent parameters for the IBM-2 Hamiltonian involved in the present study are ϵ_d , κ , χ_ν , χ_π , and κ' . In a number of microscopic and phenomenological IBM-2 calculations carried out by now, however, it has been shown [36] that a simplified form of the Hamiltonian consisting only of the \hat{n}_d , and $\hat{Q}_\nu \cdot \hat{Q}_\pi$ terms is adequate to describe the low-energy quadrupole collective states of most of the medium-heavy and heavy nuclei. Thus, in the following we investigate dependencies of the results on the parameters ϵ_d , κ , χ_ν , and χ_π concerning the bosonic interactions, while keeping the parameter κ' (for the $\hat{L} \cdot \hat{L}$ term) unchanged for each nucleus. To avoid confusions, we express from now on those IBM-2 parameters used for the parent nuclei by a subscript i , representing the initial state, and those for the daughter nuclei with a subscript f , representing the final state. Six parameters in the IBFFM-2 Hamiltonian, Γ_ν , Λ_ν , A_ν , Γ_π , Λ_π , and A_π , which are the coefficients of the boson-fermion interactions, and the parameters v_d , and v_t in the residual interaction $\hat{V}_{\nu\pi}$ are to be varied. The quasi-particle energies $\tilde{\epsilon}_{j\rho}$ in \hat{H}_F , and occupation probabilities $v_{j\rho}^2$, which appear in the boson-fermion interaction \hat{V}_{BF} , GT and Fermi operators, are kept unchanged.

Figures 4–7 show calculated $\log_{10}ft$ values of the β^+ decay of the 3_1^+ ground state of ^{68}As into the lowest

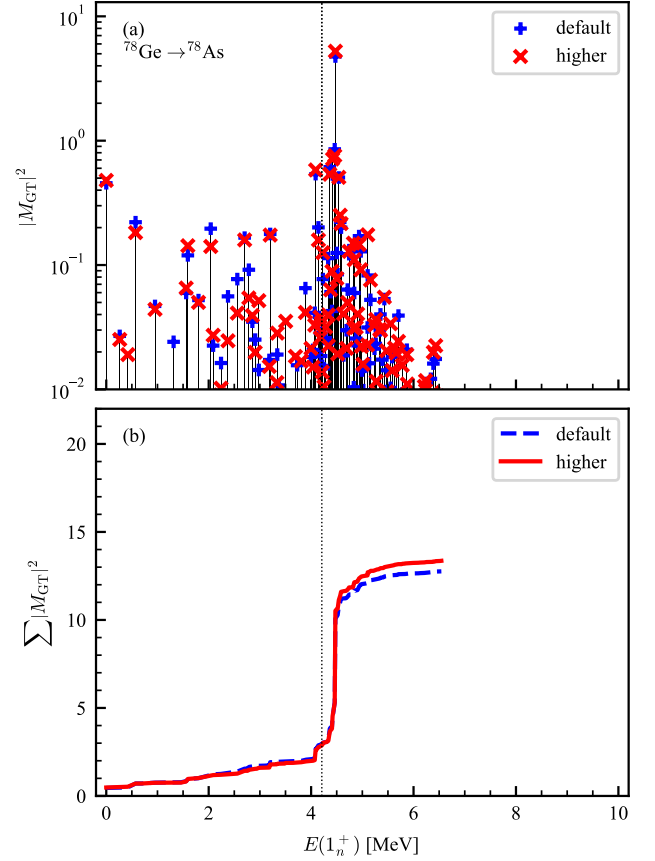


FIG. 10. Same as Fig. 8, but for the $^{78}\text{Ge}(0_1^+)$ β^- decays as functions of the excitation energies $E(1_n^+)$ of the 1^+ final states obtained from the IBFFM-2.

five 2^+ and three 4^+ states of ^{68}Ge as functions of the Hamiltonian parameters. From Fig. 4 one can see that the $\log_{10}ft$ values have little dependence on $\epsilon_{d,i}$, $\chi_{\nu,i}$ and $\chi_{\pi,i}$, which are IBFFM-2 parameters for the boson core of ^{68}As . The calculated $\log_{10}ft$ values are much more sensitive to the parameter κ_i , as they exhibit significant changes at $\kappa_i \approx -0.2$ MeV for both the $3_1^+ \rightarrow 2^+$ and $3_1^+ \rightarrow 4^+$ decays [see Figs. 4(b) and 4(f)]. The result is consistent with that obtained in our previous study on neutron-rich Zr β^- decays [35], in which the $\log_{10}ft$ values were shown to be particularly sensitive to the quadrupole-quadrupole interaction strength κ in odd-odd nuclei.

As shown in Fig. 5, the calculated $\log_{10}ft$ values are stable against variations of the boson-fermion parameters. A similar conclusion was reached in Ref. [35].

Figure 6 indicates that the predicted $\log_{10}ft$ values are constant when one varies the IBFFM-2 parameters v_t and v_d , which are interaction strengths between unpaired nucleons of the odd-odd As nuclei. This is quite at variance with the finding in Ref. [35], which showed a strong dependence of the $\log_{10}ft$ values for the Zr β^- de-

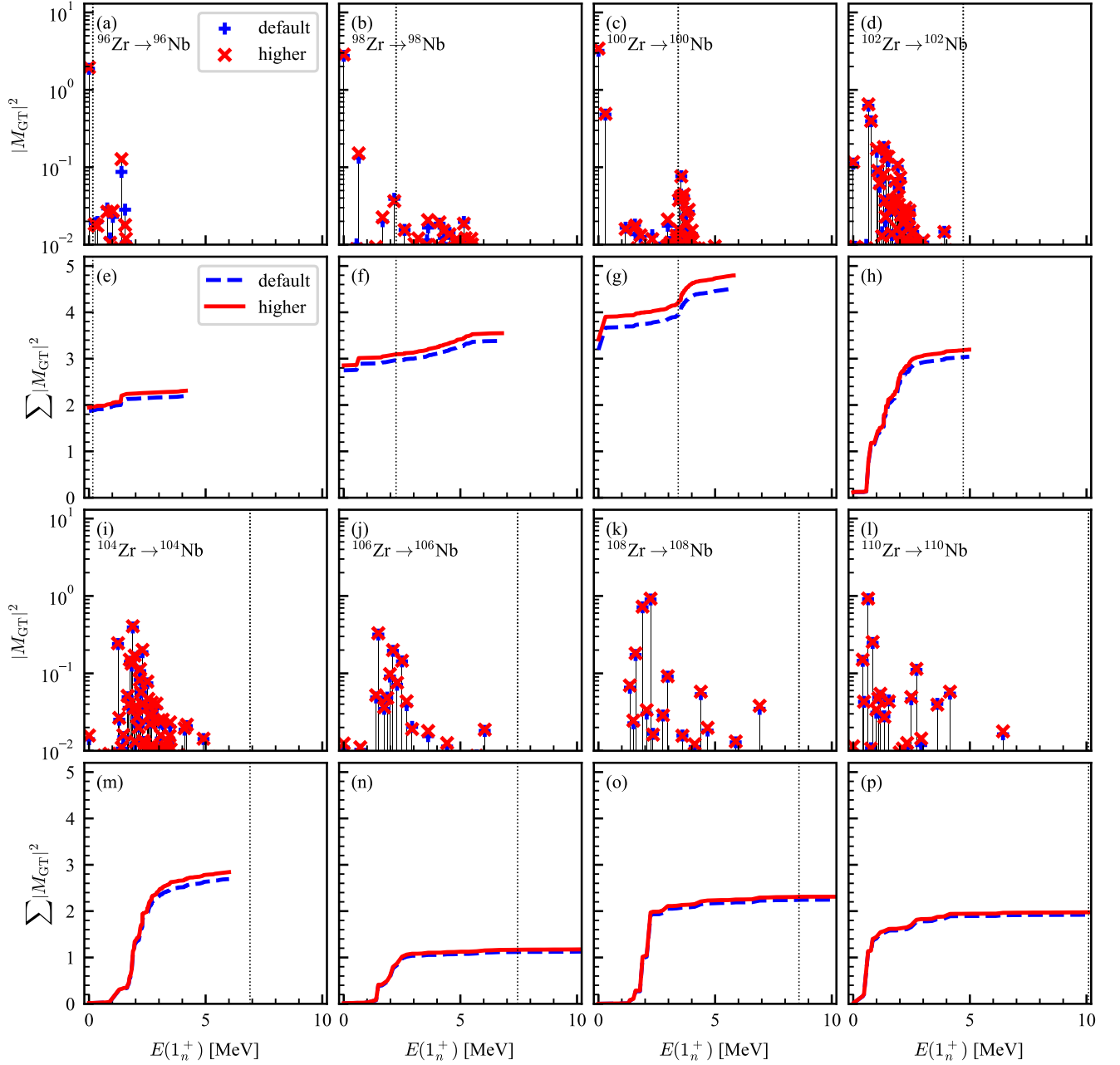


FIG. 11. Same as the Fig. 10 but for the $^{96-110}\text{Zr}(0_1^+) \beta^-$ decays.

cays on the strength parameter for the tensor interaction, v_t , of the odd-odd daughter Nb nuclei,

Figure 7 shows dependencies of the $\log_{10} ft$ values on the IBM-2 strength parameters for the daughter nucleus ^{68}Ge . One can see that the $\log_{10} ft$ values are insensitive to the parameter $\epsilon_{d,f}$. Significant changes of the $\log_{10} ft$ values for both the $3^+ \rightarrow 4^+$ and $3^+ \rightarrow 2^+$ decays with the quadrupole-quadrupole strength parameter κ_f are observed within the range $-0.05 < \kappa_f < 0$ MeV [see Figs. 7(b), and 7(f)]. For those κ_f values that are larger

in magnitude, $|\kappa_f| \gg 0.05$ MeV, the $\log_{10} ft$ values are more stable or only exhibit a gradual change with this parameter.

The $\log_{10} ft$ values also show some dependence on the parameter $\chi_{\nu,f}$, for the $3_1^+ \rightarrow 2_3^+$ and $3_1^+ \rightarrow 2_5^+$ transitions in particular [see Fig. 7(c)]. There is also something peculiar that is generally observed in the $\log_{10} ft$ systematic with the $\chi_{\nu,f}$ and $\chi_{\pi,f}$ [see Figs. 7(c), 7(d), 7(g), and 7(h)]: at particular values of these parameters anomalously large $\log_{10} ft$ values are obtained. As noted

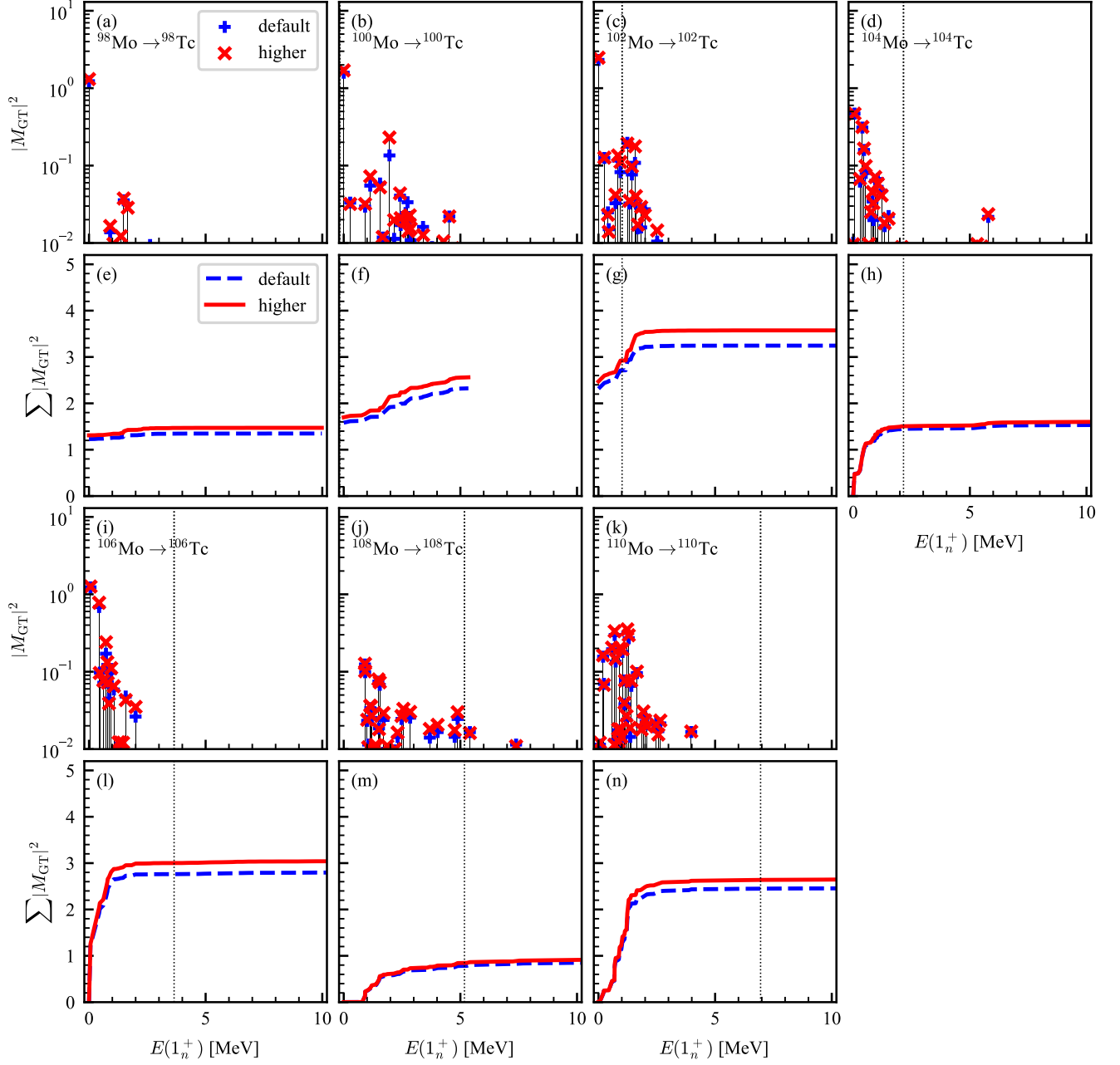


FIG. 12. Same as the Fig. 10 but for $^{98-110}\text{Mo}(0_1^+) \beta^-$ decays.

in the previous article [35], such “spike” patterns seem to occur rather accidentally, since with specific combinations of the IBM-2 as well as IBFFM-2 parameters cancellations among many different terms in the GT matrix elements occur to a great extent, leading to unexpectedly small $|M_{GT}|^2$ values, hence very large $\log_{10} ft$ values. As shown in Ref. [35], however, these peaks are not of crucial importance for our purpose, especially when we calculate the running sum $|M_{GT}|^2$ taken over large numbers of states of the final nucleus, for which the local

behaviors of $|M_{GT}|^2$ strengths do not play a role.

A major conclusion drawn from the present analysis is that the predicted $\log_{10} ft$ values for the β^+ decays of odd-odd As nuclei within the mapped IBM-2 and IBFFM-2 are especially sensitive to the quadrupole-quadrupole interaction strength κ_i in the parent or odd-odd As nuclei. This finding appears to be robust, in view of the fact that similar parameter sensitivities of the calculated $\log_{10} ft$ values were observed in our previous study of [35] for the β decays of neutron-rich Zr

region with mass $A \approx 100$. In that study, we analyzed as an illustrative example the β^- decays of the even-even $^{96-102}\text{Zr}$ isotopes, and concluded that the predicted $\log_{10} ft$ values depended significantly on the quadrupole-quadrupole interaction strength κ used for the even-even core Hamiltonian for the daughter odd-odd Nb isotopes.

C. Impacts of higher order terms on β -decay properties

We now turn to investigate possible impacts of higher-order terms in the one-nucleon transfer operators to β -decay properties. The operators in Eqs. (13) and (14) can be extended to include the additional terms

$$A_{j_\rho m_\rho}^{\dagger\prime} = A_{j_\rho m_\rho}^\dagger + \sum_{j'_\rho} \zeta'_{j_\rho j'_\rho} \left[d_\rho^\dagger \times \left(\tilde{s}_\rho \times a_{j'_\rho}^\dagger \right) \right]_{m_\rho}^{(j_\rho)} + \sum_{j'_\rho j''_\rho} \zeta_{j_\rho j'_\rho j''_\rho} \left[d_\rho^\dagger \times \left(\tilde{d}_\rho \times a_{j''_\rho}^\dagger \right)_{m'_\rho}^{(j'_\rho)} \right]_{m_\rho}^{(j_\rho)}, \quad (29)$$

$$B_{j_\rho m_\rho}^{\dagger\prime} = B_{j_\rho m_\rho}^\dagger + \sum_{j'_\rho} \theta'_{j_\rho j'_\rho} s_\rho^\dagger \left[\tilde{d}_\rho \times \left(s_\rho^\dagger \times \tilde{a}_{j'_\rho} \right) \right]_{m_\rho}^{(j_\rho)} + \sum_{j'_\rho j''_\rho} \theta_{j_\rho j'_\rho j''_\rho} s_\rho^\dagger \left[\tilde{d}_\rho \times \left(d_\rho^\dagger \times \tilde{a}_{j''_\rho} \right)_{m'_\rho}^{(j'_\rho)} \right]_{m_\rho}^{(j_\rho)}, \quad (30)$$

and their conjugate operators

$$\tilde{A}'_{j_\rho m_\rho} = (-1)^{j_\rho - m_\rho} A'_{j_\rho - m_\rho} \quad (31)$$

$$\tilde{B}'_{j_\rho m_\rho} = (-1)^{j_\rho - m_\rho} B'_{j_\rho - m_\rho}, \quad (32)$$

where the first terms on the right-hand sides of the above two equations were introduced in Eqs. (13)–(16), and are hereafter referred to as leading-order terms. Under the condition that the one-particle transition operator acts only between states that differ in generalized seniority quantum numbers by $\Delta\tilde{\nu} = \pm 1$, the coefficients of the second terms of (29) and (30), i.e., $\zeta'_{j_\rho j'_\rho}$ and $\theta'_{j_\rho j'_\rho}$, should vanish. The coefficients of the third term of Eq. (29), $\zeta_{j_\rho j'_\rho j''_\rho}$, are obtained by equating the matrix elements of the operator

$$\left[d_\rho^\dagger \times \left(\tilde{d}_\rho \times a_{j'_\rho}^\dagger \right)_{m'_\rho}^{(j'_\rho)} \right]_{m_\rho}^{(j_\rho)}, \quad (33)$$

to the corresponding ones in the shell-model (fermion) space. The coefficients $\theta_{j_\rho j'_\rho j''_\rho}$ are here assumed to be equal to $\zeta_{j_\rho j'_\rho j''_\rho}$, for the sake of simplicity. $\zeta_{j_\rho j'_\rho j''_\rho}$'s are calculated by following the procedure of Ref. [62]:

1. Construct a set of n fermion states, $|F, (i); JM\rangle$ ($i = 1, \dots, n$), and the corresponding boson states, $|B, (i); JM\rangle$ ($i = 1, \dots, n$), which are orthonormal.

2. Construct the overlap matrix Θ^J of the fermionic states for each angular momentum J . For the last term of Eq. (29), the matrix elements of Θ^J are given as

$$\Theta_{mr}^J = \delta_{mr} + 10 \left(\sum_{i=1}^n \delta_{j_i, J} \right) \times \sum_{k=1}^n \beta_{j_k j_r} \beta_{j_k j_m} \left\{ \begin{matrix} j_r & 2 & j_k \\ j_m & 2 & J \end{matrix} \right\}, \quad (34)$$

where $\beta_{j_1 j_2}$'s are defined in Eq. (6), and the curly bracket denotes Wigner's $6-j$ symbol.

3. Diagonalize the overlap matrix Θ^J

$$\Theta^J C^J = C^J \lambda^J. \quad (35)$$

Here C^J is the $n \times n$ square matrix. Its columns are the eigenvectors of Θ^J which are normalized in the condition $\sum_k (C_{ik}^J)^2 = 1$. λ^J is the diagonal matrix which contains eigenvalues of Θ^J .

4. Calculate the coefficients $\zeta_{j_\rho j'_\rho j''_\rho}$ with the expression

$$\zeta_{j_\rho j'_\rho j''_\rho} = \sum_J (-1)^{J+j_\rho+j'_\rho-j''_\rho} \times \sqrt{(2J+1)(2j'_\rho+1)} \left\{ \begin{matrix} 2 & j''_\rho & J \\ 2 & j_\rho & j'_\rho \end{matrix} \right\} \phi_{j_\rho j'_\rho}^J, \quad (36)$$

with

$$\phi_{j_\rho j'_\rho}^J = (-1)^{j_\rho - j'_\rho} u_{j_\rho} \sqrt{\frac{2J+1}{2j_\rho+1}} \times \left[\delta_{j_\rho j'_\rho} - \left\{ C^J \sqrt{\lambda^J} (C^J)^T \right\}_{k_{j_\rho} k_{j'_\rho}} \right]. \quad (37)$$

The details of the above procedure are found in Ref. [62].

The GT and Fermi operators are calculated by substituting the operators $A_{j_\rho m_\rho}^{\prime(\dagger)}$ (29) and $B_{j_\rho m_\rho}^{\prime(\dagger)}$ (30) in the formulas in Eqs. (9) and (10). Note that, in calculating the GT and Fermi matrix elements, terms that are products of more than two d -boson creation or annihilation operators are omitted, due to limitation of the current version of the computer code we have at hand. For the ^{68}As β^+ decay, for example, the code is unable to compute the matrix elements of those terms proportional to $s_\nu^\dagger \tilde{d}_\nu d_\nu^\dagger s_\pi d_\pi^\dagger \tilde{a}_{j_\nu} \tilde{a}_{j_\pi}$, $d_\nu^\dagger \tilde{d}_\pi d_\pi^\dagger \tilde{a}_{j_\nu} \tilde{a}_{j_\pi}$, and $s_\nu^\dagger \tilde{d}_\nu d_\nu^\dagger \tilde{d}_\pi d_\pi^\dagger \tilde{a}_{j_\nu} \tilde{a}_{j_\pi}$, but allows one to calculate those matrix elements that are products of any other terms in $B_{j_\nu m_\nu}^{\dagger\prime} \tilde{A}'_{j_\pi m_\pi}$ [see Eq. (17)]. New components in the matrix element of $B_{j_\nu m_\nu}^{\dagger\prime} \tilde{A}'_{j_\pi m_\pi}$ that are introduced by the inclusion of the higher-order terms are those of types $s_\nu^\dagger \tilde{d}_\pi d_\pi^\dagger \tilde{a}_{j_\nu} \tilde{a}_{j_\pi}$ and $s_\nu^\dagger d_\nu d_\nu^\dagger \tilde{a}_{j_\nu} \tilde{a}_{j_\pi}$. Note that the second terms in Eqs. (29) and (30) are omitted, since the coefficients of these terms vanish in the seniority consideration.

Figure 8 shows the GT transition strengths and their running sums for β^+ decays of $^{68}\text{As}(3_1^+)$ and $^{70}\text{As}(4_1^+)$ as functions of the excitation energy of each spin-parity state of the respective daughter nuclei. One can observe that both the GT strengths $|M_{\text{GT}}|^2$ and running sums are not significantly affected by the inclusion of the higher-order terms. An exception is that the converged value of the GT running sum for the $^{70}\text{As}(4_1^+) \rightarrow ^{70}\text{Ge}(3^+)$ β^+ decay is, by approximately a factor of 4, larger than in the calculation that takes into account up to the leading-order terms in the one-nucleon transfer operators [see Fig. 8(j)].

Figure 9 shows the Fermi transition strengths $|M_{\text{F}}|^2$ and the running sums of the $^{68,70}\text{As}$ β^+ decays. An effect of introducing the high-order terms is that, for the ^{68}As decay, the running sum $\sum |M_{\text{F}}|^2$ converges to a value that is twice as large as that obtained without the higher-order terms. As shown in Fig. 8(e), the GT sum $\sum |M_{\text{GT}}|^2$ for the β^+ decay of the 3_1^+ state of ^{68}As to the 3^+ states of ^{68}Ge is also small, and is smaller by an order of magnitude than those for the GT transitions to the 2^+ and 4^+ states of ^{68}Ge . Therefore, the β^+ decay of $^{68}\text{As}(3_1^+)$ appears to be dominated by the GT transitions to the even-spin (2^+ and 4^+) states. Compared with the dominant GT transitions, the enhancement by a factor of 2 of the Fermi strength $\sum |M_{\text{F}}|^2$ for the $3_1^+ \rightarrow 3^+$ decays by the inclusion of the high-order terms is relatively minor in the ^{68}As allowed decays. The higher-order terms, however, may have potential impacts on the predictions of processes such as the superallowed $0^+ \rightarrow 0^+$ β decays, where the GT transitions are forbidden and which are therefore determined only by the Fermi transitions. In the case of the ^{70}As decay, the present results show that the higher-order terms do not appear to have a significant influence on the Fermi transitions.

Figures 10–12 show the Gamow-Teller transition matrix elements $|M_{\text{GT}}|^2$ and their running sums for ^{78}Ge , $^{96-110}\text{Zr}$, and $^{98-110}\text{Mo}$ β^- decays, respectively, as functions of the excitation energy of 1^+ states of daughter nuclei. In all decays, the effects of the higher-order terms on the magnitude of $|M_{\text{GT}}|^2$ are small, within a few percent at most. However, there is a general trend that, for the $0_1^+ \rightarrow 1^+$ β^- decays of all the even-even nuclei, the GT sums are systematically increased by the inclusion of the higher-order terms, thus making the decay occur a little faster.

D. β -decay half lives

Using the GT and Fermi strengths obtained in the previous section, we compute the β -decay half-lives. The half-life is defined by the formula

$$T_{1/2} = \left(\sum_{0 \leq E_f \leq Q_\beta} \frac{1}{t_{1/2}^{\text{par}}} \right)^{-1}, \quad (38)$$

where Q_β stands for the β -decay Q value, which we take from experiment [57], and $t_{1/2}^{\text{par}}$ denotes the partial half-life:

$$t_{1/2}^{\text{par}} = \frac{6163}{f(Z, E_f) |M_{if}|^2}. \quad (39)$$

Here $f(Z, E_f)$ is defined as

$$f(Z, E_f) = \int_1^{E_f} dE F(Z, E) p E (E_f - E)^2 \quad (40)$$

in the units of $\hbar = m = c = 1$ [63]. E_f represents the energy difference between the ground state of the parent nucleus and the excited state of the daughter nucleus E_x , i.e., $E_f = Q_\beta - E_x$. In Eq. (40), momentum p and Fermi function $F(Z, E)$ are given as

$$p = \sqrt{E^2 - 1} \quad (41)$$

$$F(Z, E) = 2(1 + \gamma_0) \left(\frac{2pR}{\hbar} \right)^{-2(1-\gamma_0)} e^{\pi\nu} \left| \frac{\Gamma(\gamma_0 + i\nu)}{\Gamma(2\gamma_0 + 1)} \right|^2, \quad (42)$$

where

$$\gamma_0 = \sqrt{1 - (\alpha Z)^2}, \quad (43)$$

$$\nu = \pm \frac{\alpha Z E}{cp} \quad (\text{for } \beta^\mp \text{ decay}), \quad (44)$$

$$R = \frac{\alpha A^{1/3}}{2}. \quad (45)$$

with α being the fine structure constant, $\alpha = 1/137$.

By using the above formulas we compute the half-lives of the β^+ decays of $^{68,70}\text{As}$, and the β^- decays of ^{78}Ge , $^{98-110}\text{Zr}$, and $^{102-110}\text{Mo}$. Note, however, that we do not calculate the half-lives of ^{76}Ge , ^{96}Zr , and $^{98,100}\text{Mo}$ β^- decays, since they are stable nuclei, which in general do not have states satisfying the condition $0 \leq E_f \leq Q_\beta$ in Eq. (38) as the corresponding Q values are negative. The $^{72,74}\text{As}$ nuclei are unstable, and their observed ground states have spin and parity 2^- . However, since the present version of the computer code handles only the allowed (GT and Fermi) transitions, we only consider positive-parity states of these nuclei and their decays to the states of the even-even daughter $^{72,74}\text{Ge}$ of the same parity. To compute the half-lives, we use the GT and Fermi transition strengths, $|M_{\text{GT}}|^2$ and $|M_{\text{F}}|^2$, in both cases where higher-order terms are included in the corresponding one-nucleon transfer operators, and where these additional terms are not taken into account.

Figure 13 compares the predicted half-lives in the mapped IBM-2 calculations that do and do not include the higher-order terms with the experimental data. Also, Table II summarizes all the numerical values that are plotted in Fig. 13, since it is especially hard to distinguish between the predicted values by the two sets of the IBM-2 calculations in the figure. As one can see from Fig. 13, overall the calculated results show a clear trend

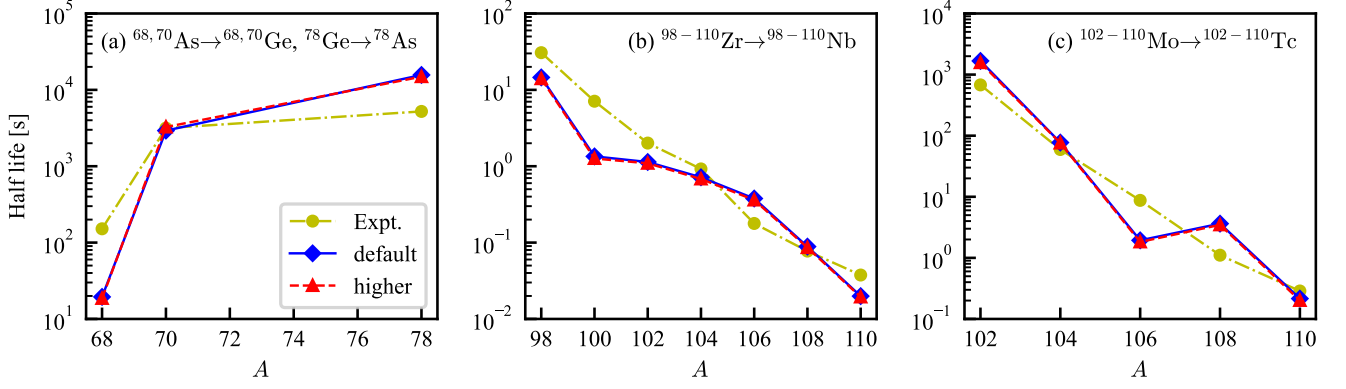


FIG. 13. Predicted β -decay half-lives that do (“higher”, red triangles) and do not (“default”, blue diamonds) include higher-order terms in the one-nucleon transfer operators. Available experimental data (“Expt.”, yellow circles) are also shown.

that half-lives become shorter as one moves away from the β -stability line to the neutron-rich side, and the order of magnitude of the calculated half-lives is also roughly consistent with data. In addition, the inclusion of the higher-order terms in the one-nucleon transfer operators is rather minor, as it changes the half-lives by approximately 5-10 % (see, Table II). One cannot, therefore, firmly conclude as to whether or not the higher-order term effects are significant enough to improve description of the β -decay half-life calculations within the present implementation of the IBM.

We now have a closer look into Fig. 13. In Table 13(a), the half-lives of $^{68}\text{As}(3_1^+) \rightarrow ^{68}\text{Ge}$ obtained from the IBM-2 calculations are, by an order of magnitude, smaller than experimental data, while the calculated half-lives of $^{70}\text{As}(4_1^+) \rightarrow ^{70}\text{Ge}$ are quite close to the experimental value. The calculated half-lives of the $^{78}\text{Ge} \beta^-$ decay are by approximately a factor of 3 larger than the experimental value. Figure 13(b) shows that the IBM-2 calculations generally underestimate the half-lives of Zr isotopes with $N \leq 62$. For the β^- -decay half-lives of the neighboring $^{102-110}\text{Mo}$ nuclei, shown in Fig. 13(c), the present calculation reproduces the observed decreasing pattern of half-lives with the neutron number reasonably well. A local irregularity or increase of the calculated half-life from ^{106}Mo to ^{108}Mo may reflect the fact that they are close to the middle of the neutron major shell $N = 66$, after which bosons in the IBM-2 are treated as holes, and therefore the number of (like-hole) bosons turns out to decrease for those neutron numbers with $N \geq 66$. It should be noted, nevertheless, that the calculated half-lives for both the ^{106}Mo to $^{108}\text{Mo} \beta^-$ decays are in the same order of magnitude as the corresponding experimental values.

TABLE II. Calculated and experimental [57] β -decay half-lives (in seconds) for those nuclei plotted in Fig. 13. The calculated results within the mapped IBM-2 that do (“Higher”) and do not (“Default”) include higher-order terms in the one-nucleon transfer operators are compared.

Parent	Daughter	Expt.	IBM-2	
			Default	Higher
^{68}As	^{68}Ge	152	19	19
^{70}As	^{70}Ge	3156	2927	3261
^{78}Ge	^{78}As	5220	15680	14886
^{98}Zr	^{98}Nb	30.7	14.5	14.0
^{100}Zr	^{100}Nb	7.1	1.3	1.323
^{102}Zr	^{102}Nb	2.01	1.14	1.09
^{104}Zr	^{104}Nb	0.922	0.716	0.681
^{106}Zr	^{104}Nb	0.178	0.378	0.361
^{108}Zr	^{108}Nb	0.0774	0.0886	0.0859
^{110}Zr	^{110}Nb	0.0376	0.0199	0.0194
^{102}Mo	^{102}Tc	678	1673	1567
^{104}Mo	^{104}Tc	59.4	77.2	75.8
^{106}Mo	^{106}Tc	8.73	1.94	1.82
^{108}Mo	^{108}Tc	1.106	3.631	3.471
^{110}Mo	^{110}Tc	0.287	0.216	0.201

IV. SUMMARY AND CONCLUSIONS

In summary, we have analyzed parameter sensitivities of the mapped IBM-2 and IBFFM-2 descriptions of the β -decay properties of neutron-deficient Ge and As isotopes, and neutron-rich Zr and Mo isotopes. Within this framework the strength parameters for the IBM-2 Hamiltonian describing even-even nuclei, single-particle energies and occupation probabilities of unpaired nucleons, necessary to build the IBFFM-2 Hamiltonian and GT and Fermi transition operators, were completely determined by using the results of the RHB-SCMF calculations employ-

ing the DD-PC1 EDF and separable pairing interaction. Only a few coupling constants of the boson-fermion interactions and residual interaction between an odd neutron and an odd proton had to be adjusted to reproduce the experimental low-energy spectra in odd-mass and odd-odd nuclei.

From the behaviors of the calculated $\log_{10}ft$ values as functions of a model parameter, it has been found that the β^+ decay of ^{68}As depends on the quadrupole-quadrupole interaction strength parameter of the parent odd-odd nucleus (i.e., ^{68}As). This finding is consistent with our previous study on the β decay of neutron-rich Zr isotopes [35], in which the quadrupole-quadrupole interaction strength parameter of odd-odd (daughter) Nb nuclei was shown to play an important role in reproducing the β -decay properties. On the other hand, at variance with the conclusion in Ref. [35] that the strength parameter for the tensor-type residual proton-neutron interaction for odd-odd nuclei is also relevant, in the present analysis the calculated β^+ -decay $\log_{10}ft$ values were shown to be almost independent of this parameter. A common feature of the mapped IBM-2 description for both the β^+ decay of ^{68}As and β^- decay of neutron-rich Zr nuclei is, therefore, that the calculated $\log_{10}ft$ values are most sensitive to the quadrupole-quadrupole interaction strength for the even-even boson core of an odd-odd nucleus, regardless of whether it is a parent or daughter nucleus of the decay process.

We further investigated effects of higher-order terms in the one-nucleon transfer operators, which are used to calculate the Gamow-Teller and Fermi operators, on the β -decay properties of As, Ge, Zr and Mo isotopes. It was found that the inclusion of the higher-order terms makes non-negligible contributions to the GT and Fermi strength distributions, their running sums, and half-lives, but does not alter the overall features of these quanti-

ties, which are characteristic of the allowed decays. The higher-order contributions may have potential impacts on the predictions of superallowed β decays, since in these processes the GT transitions are forbidden and only the Fermi ones are present. In addition, we have presented an application of the mapped IBM-2 framework to compute the β -decay half-lives that has rarely been investigated in the literature. The results shown in Fig. 13 indicate the ability of this framework to describe the overall trend and absolute values of the observed β -decay half-lives of neutron-rich nuclei. We consider the employed theoretical method as well as the reported results to be promising, given the fact that the method is largely based on the microscopic EDF calculations and thus allows for a consistent description of nuclear structures and β decay, with a minimal set of phenomenological parameters.

A possible future work could be to extend the present analysis to carry out more systematic half-life calculations, involving many other neutron-rich heavy nuclei that are experimentally of much interest. It is also feasible to extend the present parameter sensitivity analysis to the β -decay studies of odd-mass nuclei, which were not explicitly considered in the present and previous [35] studies, within the interacting boson-fermion model (IBFM-2). It is especially expected that the β -decay properties of odd-mass nuclei also depend on the relevant strength parameters, such as that for the quadrupole-quadrupole boson interaction in the IBFM-2 Hamiltonian. In the meantime, since in the current version of the employed theoretical method the strength parameters for the boson-fermion and residual neutron-proton interactions are fitted to experimental low-energy spectra, it is crucial to develop a way to derive or constrain these parameters only by the microscopic EDF calculations. Work along these lines is in progress and will be reported elsewhere.

-
- [1] I. Dillmann, K.-L. Kratz, A. Wöhr, O. Arndt, B. A. Brown, P. Hoff, M. Hjorth-Jensen, U. Köster, A. N. Ostrowski, B. Pfeiffer, D. Seweryniak, J. Shergur, and W. B. Walters (the ISOLDE Collaboration), *Phys. Rev. Lett.* **91**, 162503 (2003).
 - [2] S. Nishimura, Z. Li, H. Watanabe, K. Yoshinaga, T. Sumikama, T. Tachibana, K. Yamaguchi, M. Kurata-Nishimura, G. Lorusso, Y. Miyashita, A. Odahara, H. Baba, J. S. Berryman, N. Blasi, A. Bracco, F. Camera, J. Chiba, P. Doornenbal, S. Go, T. Hashimoto, S. Hayakawa, C. Hinke, E. Ideguchi, T. Isobe, Y. Ito, D. G. Jenkins, Y. Kawada, N. Kobayashi, Y. Kondo, R. Krücken, S. Kubono, T. Nakano, H. J. Ong, S. Ota, Z. Podolyák, H. Sakurai, H. Scheit, K. Steiger, D. Steppenbeck, K. Sugimoto, S. Takano, A. Takashima, K. Tajiri, T. Teranishi, Y. Wakabayashi, P. M. Walker, O. Wieland, and H. Yamaguchi, *Phys. Rev. Lett.* **106**, 052502 (2011).
 - [3] M. Quinn, A. Aprahamian, J. Pereira, R. Surman, O. Arndt, T. Baumann, A. Becerril, T. Elliot, A. Estrade, D. Galaviz, T. Ginter, M. Hausmann, S. Hennrich, R. Kessler, K.-L. Kratz, G. Lorusso, P. F. Mantica, M. Matos, F. Montes, B. Pfeiffer, M. Portillo, H. Schatz, F. Schertz, L. Schnorrenberger, E. Smith, A. Stolz, W. B. Walters, and A. Wöhr, *Phys. Rev. C* **85**, 035807 (2012).
 - [4] G. Lorusso, S. Nishimura, Z. Y. Xu, A. Jungclaus, Y. Shimizu, G. S. Simpson, P.-A. Söderström, H. Watanabe, F. Browne, P. Doornenbal, G. Gey, H. S. Jung, B. Meyer, T. Sumikama, J. Taprogge, Z. Vajta, J. Wu, H. Baba, G. Benzoni, K. Y. Chae, F. C. L. Crespi, N. Fukuda, R. Gernhäuser, N. Inabe, T. Isobe, T. Kajino, D. Kameda, G. D. Kim, Y.-K. Kim, I. Kojouharov, F. G. Kondev, T. Kubo, N. Kurz, Y. K. Kwon, G. J. Lane, Z. Li, A. Montaner-Pizá, K. Moschner, F. Naqvi, M. Niikura, H. Nishibata, A. Odahara, R. Orlandi, Z. Patel, Z. Podolyák, H. Sakurai, H. Schaffner, P. Schury, S. Shibagaki, K. Steiger, H. Suzuki, H. Takeda, A. Wendt, A. Yagi, and K. Yoshinaga, *Phys. Rev. Lett.* **114**, 192501 (2015).
 - [5] R. Caballero-Folch, C. Domingo-Pardo, J. Agramunt,

- A. Algora, F. Ameil, A. Arcones, Y. Ayyad, J. Benlliure, I. N. Borzov, M. Bowry, F. Calviño, D. Cano-Ott, G. Cortés, T. Davinson, I. Dillmann, A. Estrade, A. Evdokimov, T. Faestermann, F. Farinon, D. Galaviz, A. R. García, H. Geissel, W. Gelletly, R. Gernhäuser, M. B. Gómez-Hornillos, C. Guerrero, M. Heil, C. Hinke, R. Knöbel, I. Kojouharov, J. Kurcewicz, N. Kurz, Y. A. Litvinov, L. Maier, J. Marganec, T. Marketin, M. Marta, T. Martínez, G. Martínez-Pinedo, F. Montes, I. Mukha, D. R. Napoli, C. Nociforo, C. Paradela, S. Pietri, Z. Podolyák, A. Prochazka, S. Rice, A. Riego, B. Rubio, H. Schaffner, C. Scheidenberger, K. Smith, E. Sokol, K. Steiger, B. Sun, J. L. Tañ, M. Takechi, D. Testov, H. Weick, E. Wilson, J. S. Winfield, R. Wood, P. Woods, and A. Yeremin, *Phys. Rev. Lett.* **117**, 012501 (2016).
- [6] K. Langanke and G. Martínez-Pinedo, *Rev. Mod. Phys.* **75**, 819 (2003).
- [7] E. Caurier, G. Martínez-Pinedo, F. Nowacki, A. Poves, and A. P. Zuker, *Rev. Mod. Phys.* **77**, 427 (2005).
- [8] S. Yoshida, Y. Utsuno, N. Shimizu, and T. Otsuka, *Phys. Rev. C* **97**, 054321 (2018).
- [9] T. Suzuki, S. Shibagaki, T. Yoshida, T. Kajino, and T. Otsuka, *Astrophys. J.* **859**, 133 (2018).
- [10] A. Kumar, N. Shimizu, Y. Utsuno, C. Yuan, and P. C. Srivastava, *Phys. Rev. C* **109**, 064319 (2024).
- [11] P. Möller, B. Pfeiffer, and K.-L. Kratz, *Phys. Rev. C* **67**, 055802 (2003).
- [12] R. Álvarez-Rodríguez, P. Sarriguren, E. M. de Guerra, L. Paceaescu, A. Faessler, and F. Šimkovic, *Phys. Rev. C* **70**, 064309 (2004).
- [13] P. Sarriguren, *Phys. Rev. C* **91**, 044304 (2015).
- [14] J. M. Boillos and P. Sarriguren, *Phys. Rev. C* **91**, 034311 (2015).
- [15] P. Pirinen and J. Suhonen, *Phys. Rev. C* **91**, 054309 (2015).
- [16] F. Šimkovic, V. Rodin, A. Faessler, and P. Vogel, *Phys. Rev. C* **87**, 045501 (2013).
- [17] M. T. Mustonen and J. Engel, *Phys. Rev. C* **93**, 014304 (2016).
- [18] T. Marketin, L. Huther, and G. Martínez-Pinedo, *Phys. Rev. C* **93**, 025805 (2016).
- [19] J. T. Suhonen, *Frontiers Phys.* **5**, 55 (2017).
- [20] E. M. Ney, J. Engel, T. Li, and N. Schunck, *Phys. Rev. C* **102**, 034326 (2020).
- [21] A. Ravlić, E. Yüksel, Y. F. Niu, and N. Paar, *Phys. Rev. C* **104**, 054318 (2021).
- [22] K. Yoshida, Y. Niu, and F. Minato, *Phys. Rev. C* **108**, 034305 (2023).
- [23] P. Navrátil and J. Dobe, *Phys. Rev. C* **37**, 2126 (1988).
- [24] F. Dellagiacoma and F. Iachello, *Phys. Lett. B* **218**, 399 (1989).
- [25] S. Brant, N. Yoshida, and L. Zuffi, *Phys. Rev. C* **70**, 054301 (2004).
- [26] S. Brant, N. Yoshida, and L. Zuffi, *Phys. Rev. C* **74**, 024303 (2006).
- [27] N. Yoshida and F. Iachello, *Prog. Theor. Exp. Phys.* **2013**, 043D01 (2013).
- [28] E. Mardones, J. Barea, C. E. Alonso, and J. M. Arias, *Phys. Rev. C* **93**, 034332 (2016).
- [29] K. Nomura, R. Rodríguez-Guzmán, and L. M. Robledo, *Phys. Rev. C* **101**, 024311 (2020).
- [30] K. Nomura, R. Rodríguez-Guzmán, and L. M. Robledo, *Phys. Rev. C* **101**, 044318 (2020).
- [31] J. Ferretti, J. Kotila, R. I. M. n. Vsevolodovna, and E. Santopinto, *Phys. Rev. C* **102**, 054329 (2020).
- [32] K. Nomura, *Phys. Rev. C* **105**, 044306 (2022).
- [33] K. Nomura, L. Lotina, R. Rodríguez-Guzmán, and L. M. Robledo, *Phys. Rev. C* **106**, 064304 (2022).
- [34] K. Nomura, *Phys. Rev. C* **109**, 034319 (2024).
- [35] M. Homma and K. Nomura, *Phys. Rev. C* **110**, 014303 (2024).
- [36] F. Iachello and A. Arima, *The interacting boson model* (Cambridge University Press, Cambridge, 1987).
- [37] K. Nomura, N. Shimizu, and T. Otsuka, *Phys. Rev. Lett.* **101**, 142501 (2008).
- [38] K. Nomura, N. Shimizu, and T. Otsuka, *Phys. Rev. C* **81**, 044307 (2010).
- [39] K. Nomura, T. Otsuka, N. Shimizu, and L. Guo, *Phys. Rev. C* **83**, 041302 (2011).
- [40] F. Iachello and P. Van Isacker, *The interacting boson-fermion model* (Cambridge University Press, Cambridge, 1991).
- [41] S. Brant, V. Paar, and D. Vretenar, *Z. Phys. A* **319**, 355 (1984).
- [42] F. T. Avignone, S. R. Elliott, and J. Engel, *Rev. Mod. Phys.* **80**, 481 (2008).
- [43] J. Engel and J. Menéndez, *Rep. Prog. Phys.* **80**, 046301 (2017).
- [44] M. Agostini, G. Benato, J. A. Detwiler, J. Menéndez, and F. Vissani, *Rev. Mod. Phys.* **95**, 025002 (2023).
- [45] K. Nomura, *Phys. Rev. C* **105**, 044301 (2022).
- [46] K. Nomura, *Phys. Rev. C* **110**, 024304 (2024).
- [47] T. Otsuka, A. Arima, F. Iachello, and I. Talmi, *Phys. Lett. B* **76**, 139 (1978).
- [48] T. Otsuka, A. Arima, and F. Iachello, *Nucl. Phys. A* **309**, 1 (1978).
- [49] O. Scholten, *Prog. Part. Nucl. Phys.* **14**, 189 (1985).
- [50] D. Vretenar, A. V. Afanasjev, G. A. Lalazissis, and P. Ring, *Phys. Rep.* **409**, 101 (2005).
- [51] T. Nikšić, D. Vretenar, and P. Ring, *Prog. Part. Nucl. Phys.* **66**, 519 (2011).
- [52] T. Nikšić, D. Vretenar, and P. Ring, *Phys. Rev. C* **78**, 034318 (2008).
- [53] Y. Tian, Z. Y. Ma, and P. Ring, *Phys. Lett. B* **676**, 44 (2009).
- [54] J. N. Ginocchio and M. W. Kirson, *Nucl. Phys. A* **350**, 31 (1980).
- [55] K. Nomura, T. Nikšić, and D. Vretenar, *Phys. Rev. C* **93**, 054305 (2016).
- [56] K. Nomura, R. Rodríguez-Guzmán, and L. M. Robledo, *Phys. Rev. C* **99**, 034308 (2019).
- [57] Brookhaven National Nuclear Data Center, <http://www.nndc.bnl.gov>.
- [58] P. Cejnar, J. Jolie, and R. F. Casten, *Rev. Mod. Phys.* **82**, 2155 (2010).
- [59] P. D. Duval and B. R. Barrett, *Phys. Lett. B* **100**, 223 (1981).
- [60] F. Iachello, ed., *Interacting Bose-Fermi Systems in Nuclei* (Springer, New York, 1981).
- [61] F. Dellagiacoma, *Beta decay of odd mass nuclei in the interacting boson-fermion model*, Ph.D. thesis, Yale University (1988).
- [62] J. Barea, C. E. Alonso, and J. M. Arias, *Phys. Rev. C* **65**, 034328 (2002).
- [63] E. J. Konopinski and M. E. Rose, in *Alpha-Beta and Gamma-ray Spectroscopy*, Vol. 2, edited by S. Kai (North-Holland Publishing Company, Amsterdam, 1965)

p. 1327.